

Roughening Transition of a Stepped Cu(113) Surface: A Synchrotron X-Ray-Scattering Study

K. S. Liang, E. B. Sirota, K. L. D'Amico, G. J. Hughes, and S. K. Sinha

Corporate Research Science Laboratories, Exxon Research and Engineering Company, Annandale, New Jersey 08801

(Received 10 August 1987)

The study of the roughening transition of a stepped surface of Cu(113) has been performed with the use of synchrotron grazing-incidence x-ray scattering. Surface roughening was observed directly from x-ray scans of the step superlattice reflection between 300 and 750 K. The results are interpreted with a theory of Villain, Grepel, and Lapujoulade, and the values of the transition temperature, the step-step repulsive energy, and the kink energy are determined to be 620 ± 10 K, 7.4 ± 0.9 meV, and 181 ± 6.5 meV, respectively.

PACS numbers: 61.50.Ks, 64.60.Cn, 68.35.Bs, 68.35.Rh

The phenomenon of thermal roughening of a single-crystal surface has long been studied both theoretically and experimentally.¹⁻³ The equilibrium roughening of a clean smooth surface can be described in terms of thermally created atomic steps and kinks. Such surface defects, which are usually generated at elevated temperatures, often play crucial roles in important technological areas, including catalysis, crystal growth, and equilibrium crystal shape. Experimentally, much work has been devoted to finding model systems to study the nature of the roughening transition. In this respect, the vicinal (11 n) surfaces of face-centered-cubic (fcc) metals serve as possible prototypical examples for such studies, as shown recently with He-atom diffraction for Cu^{2,4} and Ni.³ In this paper, we report a synchrotron x-ray-scattering study of the roughening transition on a stepped Cu(113) surface.

The roughening transition of crystal surfaces is commonly described theoretically by a solid-on-solid model,¹ which is shown to undergo an infinite-order phase transition of the Kosterlitz-Thouless type at temperature T_r . The roughness of the surface is described by the height-height correlation function in reference to the low-temperature smooth surface. The correlation length associated with this function diverges exponentially as $T \rightarrow T_r$ and stays infinite for $T > T_r$. For vicinal fcc (11 n) surfaces, a statistical description of the thermal roughening ("meandering") of the step lines was recently given by Villain, Grepel, and Lapujoulade² based on a modified solid-on-solid model. In this model, the Hamiltonian describing the atomic picture of a rough surface assumes two interaction energies, the step-step repulsive energy w_n and the kink creation energy W_0 . Having $w_n \ll T \ll W_0$ under general experimental conditions, the theory derives the roughening transition temperature T_r from the relation,

$$(w_n/T_r) \exp(W_0/T_r) = R, \quad (1)$$

where R is a constant of order unity.²

Experimentally, although thermal roughening on these vicinal surfaces has been observed in the He-atom dif-

fraction experiments^{3,4} the nature (e.g., order, kinetics, size effect) of the phase transition has not been studied yet. It is advantageous to perform the study with x-ray techniques because, in favorable cases, the Born approximation is valid and corrections for multiple and inelastic scattering are small. For surface studies, monolayer sensitivity using the grazing-incidence x-ray-scattering technique has also been well established by the employment of high-brilliance synchrotron sources.⁵ The step roughening can therefore, in principle, be probed directly with x rays.

The Cu(113) crystal used in this UHV study was prepared by our going through a typical surface preparation procedure of mechanical polishing, prolonged annealing in flowing H₂ at 700°C, followed by electrochemical polishing. The crystal has a bulk mosaic of $\approx 0.1^\circ$ with the surface oriented to within 0.05° of the (113) normal. A clean surface with a sharp characteristic LEED pattern was observed after extensive cycles of sputtering with 500-V Ne⁺ ions and annealing at 700°C in the UHV chamber. After this stage of preparation, the quality (i.e., the long-range order and the smoothness) of the surface can only be judged from surface x-ray scans.

The x-ray study was carried out on the Exxon x-ray beamline (X10A) at the National Synchrotron Light Source. The incident-beam collimation in the vertical (in-plane surface scan) direction was determined by a double-crystal Si(111) monochromator (x-ray wavelength 1.425 Å) and the beam height was 1 mm. The sample was 8 mm in diameter and the incident angle of the beam on the surface was kept near the critical angle ($\approx 0.38^\circ$). The horizontal divergence of the incident beam was 0.1° as determined by slits and the horizontal acceptance of the scattered beam was 0.2° . The scattered measurements were performed with a newly constructed "z-axis" type diffractometer⁵ with integrated UHV surface preparation and characterization capabilities. The spectrometer resolution was adjusted to match the observed width of the surface reflections for an optimum signal-to-background ratio by use of either slits or

analyzer crystals in the diffracted beam. The best data were taken with a pyrolytic graphite analyzer crystal.

The roughening of the steps is most directly revealed in the step superlattice reflection. Typical x-ray longitudinal scans of such a reflection at different temperatures are shown in Fig. 1(a). We notice that the peak at wave-vector transfer $Q=1$ [in units of $2\pi/4.239 \text{ \AA}^{-1}$; the length 4.239 \AA corresponds to the step-step distance along the Cu(113) surface] shows strong temperature dependence. Interestingly, satellite peaks on both sides of the principal peak [Fig. 1(b)] were observed under the quenching conditions as discussed below.

We wish to stress that a step superlattice peak as shown in the figure was observed only after rigorous surface cleaning and annealing cycles. Once prepared, such an ordered stepped surface could be maintained for days inside our spectrometer chamber which had a base pressure in the mid 10^{-10} -Torr range (residual gas was primarily H_2). Despite the good quality of the observed LEED pattern, the in-plane x-ray scans showed that the surface mosaic was $\approx 2^\circ$ (FWHM) wide. Clearly related to this was the fact that our superlattice peak was finite-size limited, corresponding to a coherence length $\approx 170 \text{ \AA}$. This limited the peak intensity to ≈ 8 counts/sec.

The satellite peaks at $Q \approx 0.85$ and 1.15 as shown in Fig. 1(b) were observed as the result of quenching the

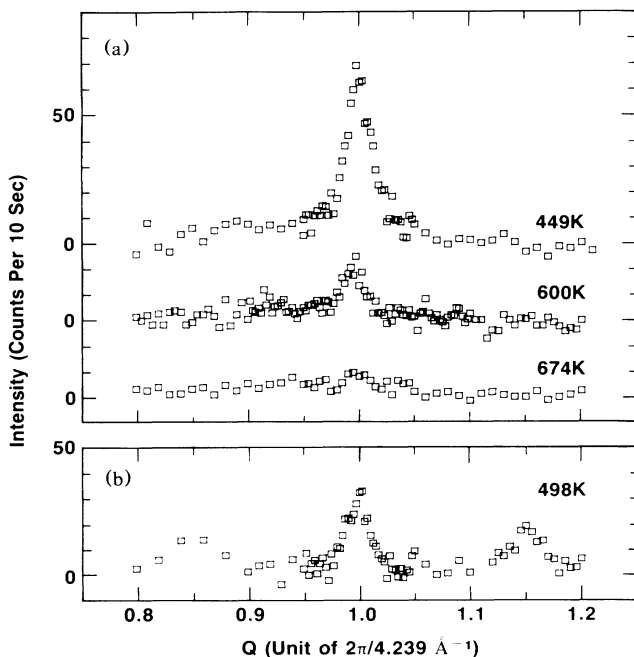


FIG. 1. (a) Longitudinal scans through the step superlattice peak with a pyrolytic graphite (001) analyzer at 449, 600, and 674 K, respectively. One can see that there is still finite intensity in the peak at 674 K. (b) A scan at 498 K after the surface had been quenched from 980 K. Notice the satellites on the sides.

surface from 980 to below 500 K. The appearance of the satellites is a signature of a modulated stepped structure. In the case shown, the structural modulation has a period equivalent to about $1/\Delta Q \approx 7$ step spacings. One possible explanation for such modulation is the presence of double-step-height edges, regularly spaced. Such edges might be formed at a temperature $T \gg T_r$, from which the surface was quenched. These satellites disappeared around 560 K when the sample was heated toward the roughening transition. The modulated structure so observed was therefore metastable and did not appear under slow-cooling conditions.

To study the step roughening, most x-ray measurements were done by our starting at 725 K, and cooling slowly to minimize kinetic effects. The transition was then observed to be quite reversible. The integrated intensity of the step superlattice peak (with the flat background subtracted) as a function of temperature is shown in Fig. 2(a). We notice that the intensity starts to

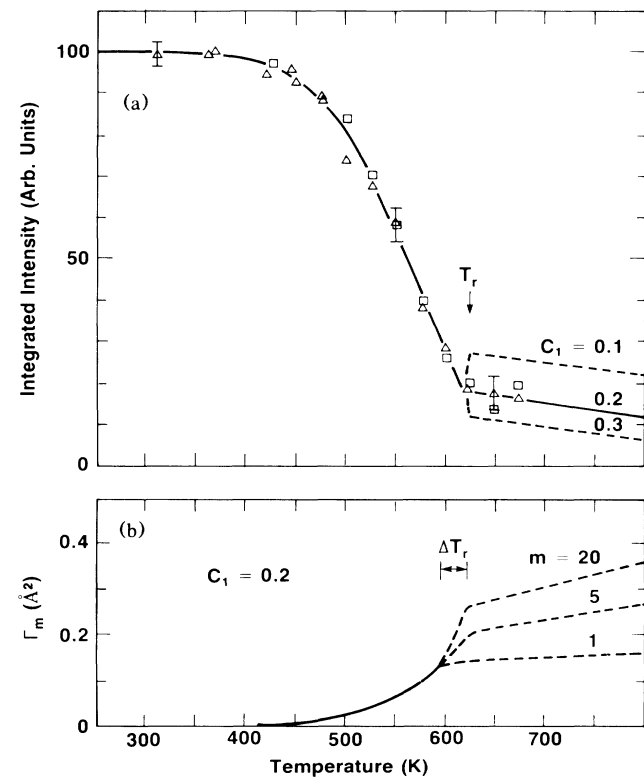


FIG. 2. (a) Integrated intensity of the step superlattice peak plotted vs temperature. Squares were taken on heating and triangles on cooling. Typical uncertainties are shown. The solid line is a fit by a form derived from Villain, Grepel, and Lapujoulade. Integration was done from $Q=0.95$ to $Q=1.05$ and "background" was computed by integration from $Q=0.85$ to 0.95 and $Q=1.05$ to 1.15 . (b) Correlation function Γ_m , in units of $a\delta/2$ ($a_0=3.615 \text{ \AA}$ for Cu), shown for representative steps with $m=1, 5,$ and 20 as a function of temperature (see text).

decrease rapidly at fairly low temperature (≈ 450 K) and levels off at $\approx 18\%$ of the low-temperature value near 620 K. The observed intensity drop is a clear indication of the onset of thermal "meandering" of the step lines. The observed leveling off of the intensity at high temperatures as shown in the figure is a direct indication of the roughening transition.

In order to discuss the x-ray-scattering intensity of the

$$S(\mathbf{q}) = \frac{C}{q_x^2} = \sum_{m=-\infty}^{+\infty} \int dy \exp\{iq_x[ml_0 + u_m(y) - u_0(0)]\} \exp(iq_y y) \exp[-(m^2 l_0^2 + y^2)\pi/L^2], \quad (2)$$

where C is a constant, l_0 is the step-step spacing, $u_m(y)$ is the meander of the m th step at position y , and L is an effective coherence size for the surface domain which includes the finite instrumental resolution. One notes that the intrastep (interstep) correlations are given in Eq. (2) by the terms with $m=0$ ($m \neq 0$). In the present experiment, the large crystal mosaic effectively integrates over q_y . Note that q_x is the longitudinal scan direction in our measurements. Assuming that u_m is a Gaussian random variable, Eq. (2) reduces to

$$S(q_x) = (C/q_x^2) \sum_m \exp(iq_x m l_0) \exp(-\frac{1}{2} q_x^2 \Gamma_m) \exp(-\pi m^2 l_0^2/L^2), \quad (3)$$

where $\Gamma_m = \langle [u_m(0) - u_0(0)]^2 \rangle$; the angular brackets denote a thermal average.

We may now calculate $S(q_x)$ using various forms of Γ_m . Here we have been guided by the expressions given by Villain, Grepel, and Lapujoulade² from a renormalization-group argument:

$$\Gamma_m = 4(T/w_n')^2 e^{-2W_0/T} a^2, \quad T \ll T_r, \quad (4a)$$

$$\Gamma_m = \{C_0 + C_1 [T/\pi(\eta\eta')^{1/2}] \ln \rho\} a^2, \quad T \geq T_r, \quad (4b)$$

where $\rho = m(\eta/\eta')^{1/4}$, $\eta = \frac{1}{2} T \exp(W_0/T)$, $\eta' = w_n$, a is the unit distance ($= a_0/\sqrt{2}$, a_0 is the unit-cell dimension) in the x direction to move one atomic spacing in the terrace, and C_0 and C_1 are constants to be determined in the fitting of experimental data. Here T , w_n , and W_0 are the temperature, the step-step interaction energy, and the kink formation energy, respectively, which satisfy Eq. (1). [We use a value of $\pi^2/2$ for the constant R in Eq. (1); see Ref. 2.] w_n' is the low-temperature value of the step-step interaction energy which can be different from w_n in the renormalization. Using these expressions, the integrated intensities may be calculated from Eq. (3). For T far below T_r , $S(q_x)$ will show a δ -function peak at $q_x = 2\pi/l_0$ [$l_0 = \sqrt{11}a/2 = 4.239$ Å for the Cu(113) surface], while only diffuse scattering exists above T_r . Equation (3) was integrated over the same q range used in the analysis of the experimental data, and the "background," over the q range used to estimate the latter. The difference between the two was then fitted to the intensity data shown in Fig. 2(a).

In fitting the intensity data with the above expressions, the following conditions were employed to determine the values of constants C , C_0 , and C_1 . The constant C_0 , which arises from short-wavelength fluctuations, was determined by matching Γ_1 at T_r . For a given effective domain size (≈ 170 Å, or $l_0/L \approx 0.025$), the constants C and C_1 were then determined by our matching the ob-

step superlattice reflection, let us define axes such that the y axis is parallel to the steps, the x axis is in the macroscopic crystal surface, normal to the steps, and the z axis is normal to the crystal surface. When the incident and scattered beams are close to the critical angle, the component of wave-vector transfer normal to the surface is very small. Under such conditions, the Born approximation for the x-ray-scattering function $S(\mathbf{q})$ yields

served and calculated intensities, according to Eq. (3). The results of the fitting are shown in Fig. 2(a) with the parameters $w_n' = 86 \pm 10$ K, $W_0 = 2100 \pm 75$ K, $T_r = 620 \pm 10$ K, and different values of the constant C_1 , with the value $C_1 = 0.20$ for best fit. The corresponding values of Γ_m calculated from Eq. (4) are shown in Fig. 2(b), which illustrates the fact that Γ_m is independent of m for $T < T_r$ and increases logarithmically with m for $T \geq T_r$. The value of Γ_m for $m \leq 5$ at T_r is $\approx 0.45a$ ($= 1.15$ Å), which is much larger than the corresponding value (0.15 Å) estimated from the bulk Debye-Waller factor of Cu. We do not believe that in-plane deviations are much affected by the use of the (larger but not accurately known) surface Debye-Waller factor.

It should be pointed out that in the interpretation of our intensity data, we employed expressions of Ref. 2 for Γ_m for $T \ll T_r$ [Eq. (4a)] and $T \geq T_r$ [Eq. (4b)], but ignored the expression for the critical regime $T \leq T_r$ [Eq. (52) of Ref. 2]. We believe that this regime is not easily observable in the present experiment because of the finite size of the surface domains. In fact, from the quality of the fit, we judge that the "critical regime" [ΔT , in Fig. 2(b)] has a width of ≤ 20 K.

There is little doubt that the Cu(113) surface undergoes a roughening transition at relatively low temperature ($\approx 0.46T_m$) with respect to the bulk melting temperature ($T_m = 1356$ K). Our measured value of T_r for Cu(113) is in the range as predicted on phenomenological arguments³ and from a Monte Carlo simulation.⁶ The values of w_n' , W_0 , and T_r as determined are consistent with Eq. (1), within experimental and theoretical uncertainties, indicating that the temperature effect on the step-step interaction energy is weak. From a recent x-ray study of the Cu(110) surface,⁷ we also note that the thermal roughening of both Cu(113) and Cu(110) behaves according to Eq. (4a) for $T < T_r$, and a similar

value of W_0 was obtained in both cases. However, diffuse scattering (or the roughening transition) was not observed in the latter. Finally, we note that our values of w_n , W_0 , and T_r for Cu(113) are quite different from those ($w_n=560$ K, $W_0=800$ K, $T_r=720$ K) recently obtained from the He diffraction experiment.⁴ In the He diffraction, uncertainties could well arise from inelastic and multiple scattering and the finite-size effect of the sample.³

So far our discussion of the step roughening has been centered mainly on the step superlattice reflection. We also observed increased roughening from measured diffuse scattering in the vicinity of the surface truncation rod⁸ originating from the $(\bar{1}\bar{1}1)$ Bragg peak at temperature above T_r , but our results⁹ in these measurements are less quantitative as a result of the broad surface mosaic of the sample. Such x-ray studies can be performed in more detail when a higher-quality surface with better surface mosaic becomes available. In such a case, the regime near the critical temperature can be probed in detail with x-ray measurements to determine whether it is truly of the Kosterlitz-Thouless type.

In conclusion, we have performed surface x-ray-scattering measurements on a stepped surface of Cu(113) in a temperature range of 300 to 750 K. The measured temperature dependence of the step superlattice reflection shows directly the roughening transition, and the observed features can be explained quantitatively by a step roughening-transition theory given recently by Villain, Grepel, and Lapujoulade.² A step-roughening transition temperature of 620 ± 10 K, a step-step repulsive interaction of 86 ± 10 K (7.4 ± 0.9 meV), and a kink energy of 2100 ± 75 K (181 ± 6.5 meV) are determined for the Cu(113) surface.

We thank R. Hewitt and other Exxon beamline staff for excellent technical assistance. We also wish to thank W. N. Unertl for help in the experiment. The National Synchrotron Light Source is supported by the Divisions of Material Sciences and Chemical Science under Department of Energy Contract No. DE-AC02-76CH-00016.

¹S. T. Chui and J. D. Weeks, *Phys. Rev. B* **14**, 4976 (1976); for a review, see J. D. Weeks, in *Ordering in Strongly Fluctuating Condensed Matter Systems*, edited by T. Riste (Plenum, New York, 1980), p. 293.

²J. Villain, D. R. Grepel, and J. Lapujoulade, *J. Phys. F* **15**, 809 (1985).

³M. den Nijs, E. K. Riedel, E. H. Conrad, and T. Engel, *Phys. Rev. Lett.* **55**, 1698 (1985), and **57**, 1279(E) (1986); E. H. Conrad *et al.*, *J. Chem. Phys.* **84**, 1015 (1986), and **85**, 4756(E) (1986).

⁴F. Fabre, B. Salanon, and J. Lapujoulade, in *Proceedings of the Second International Conference on the Structure of Surfaces*, Amsterdam, The Netherlands, 1987 (to be published); F. Fabre *et al.*, *J. Phys. (Paris)* **48**, 1017 (1987).

⁵P. Eisenberger and W. C. Marra, *Phys. Rev. Lett.* **46**, 1081 (1981). For a review of grazing-incidence surface x-ray scattering, see P. H. Fuoss, K. S. Liang, and P. Eisenberger, in "Synchrotron Radiation Research: Advances in Surface Science," edited by R. Z. Bachrach (Plenum, New York, to be published).

⁶W. Selke and A. M. Szpilka, *Z. Phys. B* **62**, 381 (1986).

⁷S. G. J. Mochrie, *Phys. Rev. Lett.* **59**, 304 (1987).

⁸J. R. Andrews and R. A. Cowley, *J. Phys. C* **18**, 6427 (1985); I. K. Robinson, *Phys. Rev. B* **33**, 3830 (1986).

⁹K. S. Liang, E. B. Sirota, K. L. D'Amico, G. J. Hughes, S. K. Sinha, and W. N. Unertl, in Ref. 4.